



**Hydrophobicity May Enhance Membrane Affinity and Anti-Cancer Effects of Schiff Base Vanadium(V) Catecholate Complexes**

Journal:	<i>Dalton Transactions</i>
Manuscript ID	DT-ART-02-2019-000601.R1
Article Type:	Paper
Date Submitted by the Author:	08-Mar-2019
Complete List of Authors:	Crans, Debbie; Colorado State University, Chemistry Department Koehn, Jordan; Colorado State University, Chemistry Department Petry, Stephanie; Colorado State University, Chemistry Department Glover, Caleb; Colorado State University, Chemistry Department Wijetunga, Asanka; University of Sydney, School of Chemistry Kaur, Ravinder; University of Sydney, School of Chemistry Levina, Aviva; The University of Sydney, School of Chemistry Lay, Peter; The University of Sydney, School of Chemistry, F11



## Hydrophobicity May Enhance Membrane Affinity and Anti-Cancer Effects of Schiff Base Vanadium(V) Catecholate Complexes

Debbie C. Crans,<sup>\*a,b</sup> Jordan T. Koehn,<sup>a</sup> Stephanie M. Petry,<sup>a</sup> Caleb M. Glover,<sup>a</sup> Asanka Wijetunga,<sup>c</sup> Ravinder Kaur,<sup>c</sup> Aviva Levina,<sup>c</sup> and Peter A. Lay<sup>\*c</sup>

Received 00th January 20xx,  
Accepted 00th January 20xx

DOI: 10.1039/x0xx00000x

www.rsc.org/

Anti-cancer activities of vanadium compounds have generated recent interest because of a combination of desirable properties for chemotherapy, i.e., strong cytotoxicities, anti-metastatic activities and relatively low systemic toxicities. Certain hydrophobic vanadium(V) Schiff base/catecholate compounds, which as shown herein, have increased stability in aqueous media and affinity for membrane interfaces. Depending on their hydrophobicity, they may be able to enter cells intact. In this manuscript, two hydrophobic V(V) catecholate substituted analogues, [VO(Hshed)(cat)] and [VO(Hshed)(dtb)], (Hshed = *N*-(salicylideneaminato)-*N'*-(2-hydroxyethyl)-1,2-ethanediamine, cat = pyrocatechol, and dtb = 3,5-di(*tert*-butyl)catechol and the vanadium(V) precursor [V(O)<sub>2</sub>(Hshed)] were synthesized for their ability to interact with membranes and their anti-cancer effects. Using <sup>51</sup>V and <sup>1</sup>H NMR spectroscopy, the presence and location of the free ligand, H<sub>2</sub>shed, and the three V(V) complexes were examined in a model membrane microemulsion system. The stability of the three complexes were measured in aqueous solution, cell media and an inhomogeneous microemulsion system. Our results demonstrated that free ligand H<sub>2</sub>shed and the intact V(V) complexes associated with the interface but that the V-complexes hydrolyzed to some extent because oxovanadates were observed by <sup>51</sup>V NMR spectroscopy and decreasing complex by absorption spectroscopy in cell media. When determining the effects of V(V) catecholate complexes on bone cancer cells, the strongest effects were observed with the more stable hydrophobic complex ([VO(Hshed)(dtb)]) that was able to best associate and penetrate the model membrane system intact. These studies would be consistent with the membrane permeability studies being a good predictor for *in vitro* cytotoxicity assays because the [VO(hshed)(dtb)] can pass through the cellular membrane intact which may enhance its anti-cancer activities.

### Introduction

Medicinal applications of metal complexes in the past has been dominated by the anti-cancer platinum drugs, as well as a range of complexes used for imaging diagnostics and nuclear medicinal applications.<sup>1-7</sup> However, several additional metal-based classes of complexes have been of interest for decades and are increasing in importance. Vitamins and nutritional additives often include metal-ion containing supplements.<sup>8-12</sup> The large number of different formulations for iron and vanadium are testament to the existence of a range of methodologies that can be applied to increase the efficacy of absorption.<sup>13</sup> Furthermore, Lipinski's rules<sup>14</sup> based on an empirical and statistical evaluation of efficacy suggest that statistically successful drugs are of certain size, hydrophobicity, polarity, or reactivity, which thus limits the chemical space to

search for available drugs. However, some of the more successful drugs do not follow these empirical rules, such as cisplatin and aspirin; therefore, drug and supplement design continues to include the entire chemical space. For example, recent investigations have introduced promising hydrophobic titanium and vanadium drugs.<sup>15-19</sup> The water solubility of these compounds and other hydrophobic drugs is very limited, and as a result, the methods for *in vivo* studies with these compounds involve dissolving the compounds in methanol, ethanol, or DMSO or dissolution in assays containing surfactants and/or DMSO. In this work, we examine the solubility, stability, and interactions of representative hydrophobic metal complexes (Fig. 1) and free ligand H<sub>2</sub>shed with a model membrane interface and their anti-cancer effects.

Identification of inhibitors for signal transduction remains an important target in drug discovery. Phosphatase inhibitors that are particularly potent, or effective in animal studies, include a series of titanium, vanadium, and zinc coordination complexes.<sup>17, 20-24</sup> In several studies,<sup>25-28</sup> series of compounds were tested, and a correlation with hydrophobicity and stability with potency was highlighted, for example, see a representative compound in Fig. 1g.<sup>26</sup> The Tshuva group used this approach with vanadium compounds and prepared a hydrophobic vanadium complex (Fig. 1h), which was found to have anti-cancer properties as well.<sup>25</sup> The high hydrophobicity of these

<sup>a</sup> Chemistry Department, Colorado State University, Fort Collins, Colorado 80523, United States.

<sup>b</sup> Cell and Molecular Biology Program, Colorado State University, Fort Collins, Colorado 80523, United States.

<sup>c</sup> School of Chemistry, The University of Sydney, Sydney, NSW 2006, Australia.

† This contribution was submitted to the special issue prepared after the 7<sup>th</sup> EuCheMs Conference on Nitrogen Ligands, Fall 2018.

Electronic Supplementary Information (ESI) available: Figure S1: 1D <sup>1</sup>H NMR spectra of [VO(Hshed)(cat)] in D<sub>2</sub>O, DMSO and Reverse Micelles; Figure S2: 1D <sup>1</sup>H NMR spectra of [VO(Hshed)(dtb)] in D<sub>2</sub>O, DMSO, and Reverse Micelles; Dynamic Light Scattering Data. See DOI: 10.1039/x0xx00000x

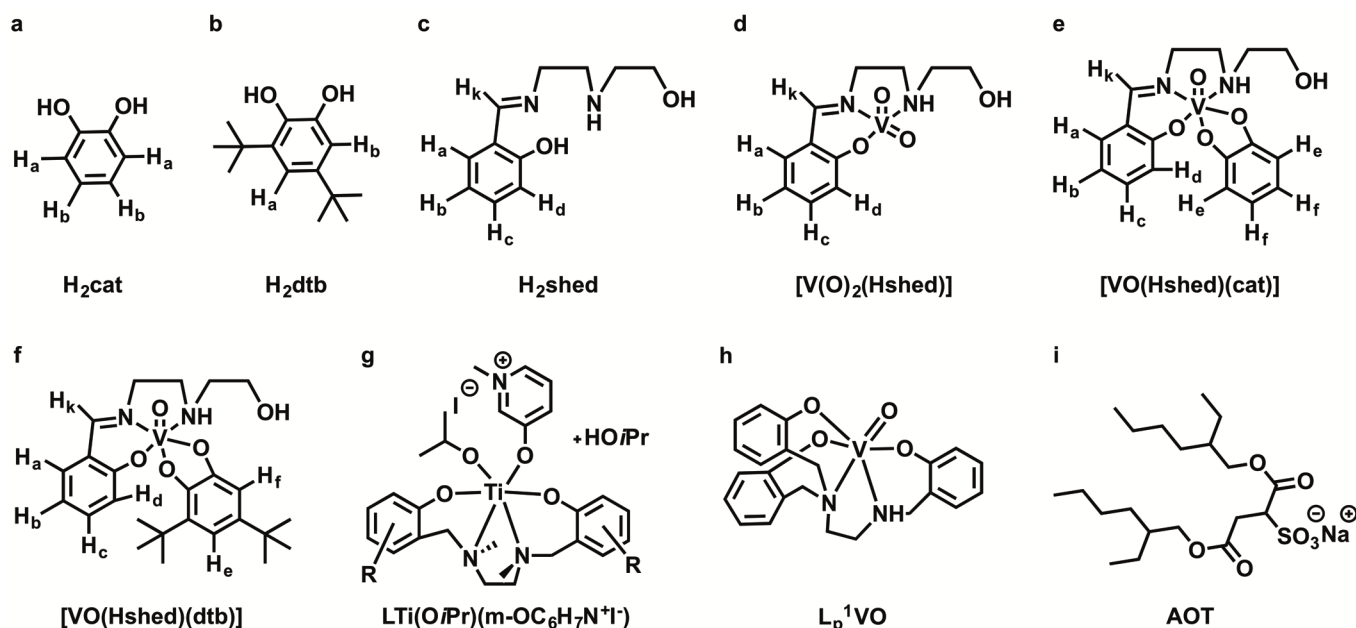


**Fig. 1** The structures are labelled as follows: (a)  $H_2cat$ ; (b)  $H_2dtb$ ; (c)  $H_2shed$ , (d)  $[V(O)_2(Hshed)]$ , (e)  $[VO(Hshed)(cat)]$ , (f)  $[VO(Hshed)(dtb)]$ , (g) Example of a hydrolytically stable titanium complex,<sup>26</sup> (h) Example of a hydrolytically stable vanadium complex,<sup>25</sup> and (i) AOT.

compounds tend to protect the complexes against initial hydrolysis making them more likely to penetrate membranes and extend their lifetime and get into cells intact. An example of such a compound is shown in Fig. 1h; a vanadium complex that was more effective in growth inhibition than cisplatin of human colon HT-29 and ovarian OVCAR-3 cells.<sup>25</sup> Studies using data mining of vanadium-containing phosphatase complexes<sup>24</sup> and synchrotron studies indicate most vanadium complexes lose their ligands when binding to phosphatases<sup>24</sup> or transferrin,<sup>29</sup> in blood, and in cell medium.<sup>30-37</sup> In contrast, these same complexes interact with human serum albumin and in some cases can form a protein adduct that maintains the ligands.<sup>37-39</sup> It is possible that complexes containing hydrophobic ligands with steric hindrance preventing substitution reactions may enable uptake of the intact complex and delivery to the cellular target and thus be a particularly potent cytotoxin to breast and pancreatic cancer cells.<sup>40</sup>

To explore how these hydrophobic complexes will interact with membrane interfaces, we have investigated the behavior of V(V) complexes with an ideal representation of a simple microemulsion ternary model membrane system shown in Fig. 2.<sup>41, 42</sup> The reverse micelle (RM) is a ternary system,  $H_2O/AOT/organic\ solvent$ , where AOT = sodium bis[2-ethylhexyl]sulfosuccinate, is used as a simple but effective model system to explore the ability of these hydrophobic coordination complexes to penetrate the interface, Fig. 2. These self-assembled structures form in a region of the phase diagram where there is little  $H_2O$ , but significant amounts of surfactant and organic solvent.<sup>43-47</sup> The interface system is dynamic, but the overall stability of the system is overall governed by thermodynamic considerations rather than kinetic ones and, thus, the most thermodynamically stable arrangements are

preserved. In the past, we have used mainly *iso*-octane or cyclohexane (or  $d_{16}$ -cyclohexane) as the organic solvent<sup>48</sup>, but others have used pentane, benzene, chloroform, and carbon tetrachloride.<sup>49</sup> The microemulsion forms RMs, but the interfacial chemistry enables studies of how such metal complexes will transverse interfaces<sup>50, 51</sup> and NMR spectroscopy provides evidence on whether the complexes decompose and where they interact with the interfaces in this simple model system.

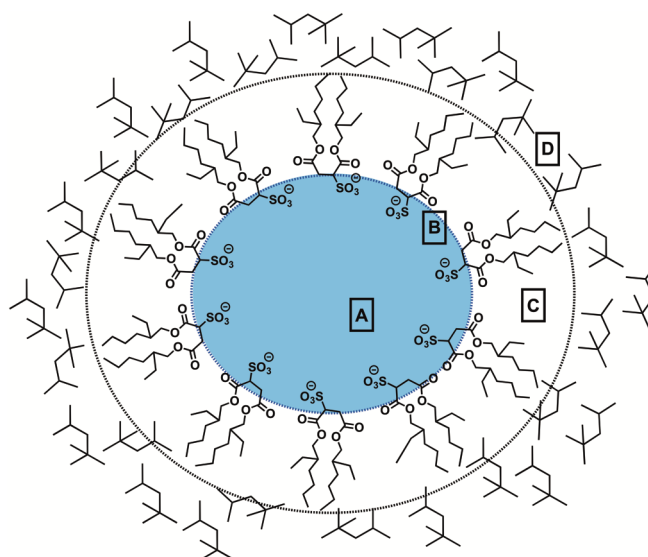


**Fig. 2** Schematic diagram of an RM present in a microemulsion. The four distinct locations for potential solutes are labelled as follows: (a) the water pool, (b) the Stern layer, (c) the surfactant hydrophobic layer, and (d) the organic solvent layer, *iso*-octane.

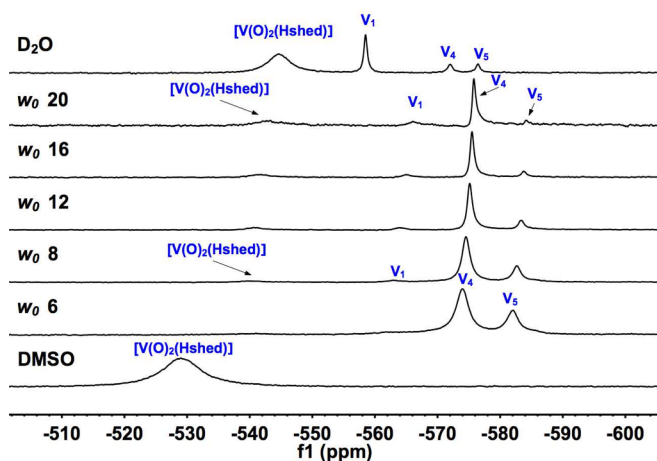


**Fig. 3**  $^{51}\text{V}$  NMR spectra of  $[\text{V}(\text{O})_2(\text{Hshed})]$  in  $\text{D}_2\text{O}$  and in a series of RMs ( $w_0 = 6, 8, 12, 16$  and  $20$  prepared from a  $0.750\text{ M}$  AOT/*iso*-octane stock solution). The spectra were recorded after equilibration was reached after 20 min for  $\text{D}_2\text{O}$  samples and after 40 min in RM samples. The pH for  $\text{D}_2\text{O}$  and RMs was 6.6 and the pD was 7.0. The total V-concentration for the  $1.0\text{ mL}$   $[\text{V}(\text{O})_2(\text{Hshed})]$  RM samples are as follows:  $w_0 20$ ,  $2.41\text{ mM}$ ;  $w_0 16$ ,  $5.17\text{ mM}$ ;  $w_0 12$ ,  $11.05\text{ mM}$ ;  $w_0 8$ ,  $23.53\text{ mM}$ ; and  $w_0 6$ ,  $36.72\text{ mM}$ .

Studies with the  $\text{BMOV}/\text{VO}_2(\text{ma})^{2-}$  system<sup>52</sup> and the V-dipic systems have demonstrated remarkable differences in how even simple compounds interact with model membrane systems. The  $\text{BMOV}/\text{VO}_2(\text{ma})^{2-}$  compounds hydrolyze as they approach the interface,<sup>52</sup> whereas the V-dipic complexes react differently depending on the oxidation state.<sup>53</sup> The V(V) complex  $[\text{VO}_2\text{dipic}]^-$  is able to penetrate the interface, whereas the V(III) complex  $[\text{V}(\text{dipic})_3]^-$  is found in the water pool associating with the interface.<sup>53</sup> The V(IV)-dipic system can form two complexes a neutral 1:2 complex  $[\text{VO}_2\text{dipic}]^-$  that is generally prepared upon synthesis as well as a 1:1 complex  $[\text{VO}(\text{H}_2\text{O})_2\text{dipic}]^-$ . The former readily associates with the interface partially penetrating the surface, whereas the 1:1 complex is interacting further up in the hydrophobic part of the interface similarly to the V(V)-dipic complex. These studies demonstrate the versatile modes of actions of these complexes,<sup>54, 55</sup> and considering that V-complexes are known to cycle between redox states in the biological systems this factor undoubtedly is involved in the mode of action of the vanadium complexes.<sup>10, 12, 19, 54-58</sup> Indeed, the redox chemistry of vanadium compounds is likely to be associated with the generation of reactive oxygen species (ROS), which have been implicated in the mode of action of vanadium compounds. This topic is beyond the scope of this manuscript and we refer the reader elsewhere on more information on this important topic.<sup>54, 55</sup>

Using this simple model membrane system, the chemistry of the ternary V(V) complex  $[\text{V}(\text{O})_2(\text{Hshed})]$  and two more hydrophobic analogs prepared from its complexation with catecholate (cat) or di-*tert*-butylcatecholate (dtb) (Fig. 1). These compounds belong to the family of complexes formed from non-innocent ligands, and as a result, exhibit a broad spectrum

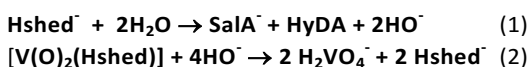
of redox chemistry.<sup>59</sup> It is well known that V-compounds redox cycle upon administration, and a number of studies have been done exploring the details of these processes. Because we focus on V(V) compounds in this study, we refer readers elsewhere on this important topic. For the V-catecholate complexes described in this work, the redox chemistry is mainly metal centred.<sup>59</sup> There have only been a few studies with vanadium-catechol complexes exploring their biological activities.<sup>60-63</sup> A recent study demonstrated that these compounds affected cell growth in MDA-MB-231 and PANC-1 cells with varying amounts of effectiveness.<sup>40</sup> Furthermore, a number of vanadium compounds have been reported with naturally occurring non-polar flavonoids including mechanistic studies probing the redox chemistry involved in these processes.<sup>64</sup> It is, therefore, important to investigate how these hydrophobic complexes interact in interface model systems to explore how this may impact their anti-cancer activities.

## Results

**Synthesis.**  $[\text{V}(\text{O})_2(\text{Hshed})]$ ,  $[\text{VO}(\text{Hshed})(\text{cat})]$ , and  $[\text{VO}(\text{Hshed})(\text{dtb})]$  and free ligand  $\text{H}_2\text{shed}$  were synthesized as previously described and the spectroscopic data was found to be consistent with that in literature.<sup>65-67</sup> The free ligand,  $\text{H}_2\text{shed}$ , is the condensation product of salicylaldehyde (SaLA) and *N*-(2-hydroxyethyl)-1,2-ethanediamine ( $\text{NH}_2\text{CH}_2\text{CH}_2\text{NHCH}_2\text{CH}_2\text{OH}$ , abbreviated HyDA).

**Solubility of Free Ligands and V(V) Complexes and Stability of Free Ligand  $\text{H}_2\text{shed}$  and  $[\text{V}(\text{O})_2(\text{Hshed})]$  in RM Samples.** The three free ligands (Hshed and cat and dtb catechols) were all dissolved in aqueous solution and *iso*-octane. The three complexes,  $[\text{V}(\text{O})_2(\text{Hshed})]$ ,  $[\text{VO}(\text{Hshed})(\text{cat})]$ , and  $[\text{VO}(\text{Hshed})(\text{dtb})]$  are all soluble in DMSO dimethylsulfoxide, but have less solubility in aqueous solution and no measurable solubility in *iso*-octane (2,2,4-trimethylpentane) as confirmed by NMR spectroscopy. All three complexes had to be forced into aqueous solvents such as  $\text{D}_2\text{O}$  via vortexing and at that point the Schiff base ligand is subjective to hydrolysis as shown in eq. (1) and the  $[\text{V}(\text{O})_2(\text{Hshed})]$  complex as shown in eq. (2).

The stability of the precursor V(V) complex,  $[\text{V}(\text{O})_2(\text{Hshed})]$ , was measured in aqueous solution prior to the addition to the model membrane RM microemulsion system. We observed that the vanadium complexes hydrolyzed as shown in eq. (2) at a faster rate in aqueous solution than in the RM mixture. Due to the presence of the Schiff base in the ligand, once the complex hydrolyzed, the ligand could continue to fragment into salicylaldehyde (SaLA) and *N*-(2-hydroxyethyl)-1,2-ethanediamine (HyDA) as shown in eq. (1) below. The equilibrium mixture of both the ligand and  $[\text{V}(\text{O})_2(\text{Hshed})]$  complex in aqueous solution was reached as evident by the NMR spectra recorded.



Once the equilibrium mixture of  $\text{H}_2\text{shed}$  ligand had been reached in aqueous solution, the solution was added to form

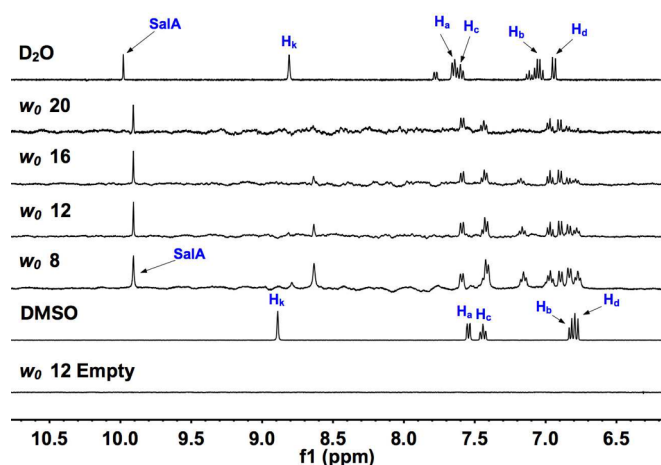


**Fig. 4**  $^1\text{H}$  NMR spectra of  $[\text{V}(\text{O})_2(\text{Hshed})]$  in  $\text{D}_2\text{O}$  and in a series of RMs ( $w_0 = 8, 12, 16,$  and  $20$  prepared from  $0.750 \text{ M}$  AOT/*iso*-octane stock solution. The spectrum in  $\text{D}_2\text{O}$  was recorded after 20 min and the RM spectra were recorded after 40 min once equilibrium had been established. SalA = salicylaldehyde. The pH for  $\text{D}_2\text{O}$  and RMs was 6.6 and the pD was 7.0. The total V-concentration for the  $1.0 \text{ mL}$   $[\text{V}(\text{O})_2(\text{Hshed})]$  RM samples are as follows:  $w_0 20, 2.41 \text{ mM}$ ;  $w_0 16, 5.17 \text{ mM}$ ;  $w_0 12, 11.05 \text{ mM}$ ;  $w_0 8, 23.53 \text{ mM}$ ; and  $w_0 6, 36.72 \text{ mM}$ .

RMs from two concentrations of AOT/*iso*-octane stock solution ( $0.200$  and  $0.750 \text{ M}$ ). Since the highest resolution  $^1\text{H}$  NMR spectra were obtained using  $0.750 \text{ M}$  AOT stock solution, the rest of the studies were carried out using this stock solution concentration (see below).  $^{51}\text{V}$  NMR spectra recorded for the precursor complex  $[\text{V}(\text{O})_2(\text{Hshed})]$  in  $\text{D}_2\text{O}$  confirmed that it hydrolyzed in aqueous solution, and that equilibrium was reached by 20 min after sample preparation (see below). Compared to the aqueous solution, the equilibrium reaction was reached slower in RMs and the equilibrium concentration was achieved after 40 min. These studies provided the time-scale of the experiments of the precursor  $[\text{V}(\text{O})_2(\text{Hshed})]$  complex sample and provided guidelines for the timeframe of the studies with this complex as well as the vanadium complexes with the catechol ligands studied where the lower solubility is problematic, which causes issues with detecting the complex.

**$^{51}\text{V}$  NMR spectra of the  $[\text{V}(\text{O})_2(\text{Hshed})]$  Complex.** In aqueous solutions, the equilibrium concentration of  $[\text{V}(\text{O})_2(\text{Hshed})]$  is about 60% of the total vanadium.  $^{51}\text{V}$  NMR spectra of  $[\text{V}(\text{O})_2(\text{Hshed})]$  in DMSO,  $\text{D}_2\text{O}$ , and in a series of RMs ( $w_0 = 6, 8, 12, 16$  and  $20$  prepared from  $0.750 \text{ M}$  AOT/*iso*-octane stock solution) are given in Fig. 3. Upon placement into the RM, the stability ratio was changed significantly and that the amount of  $[\text{V}(\text{O})_2(\text{Hshed})]$  complex in the RM environment is much smaller than in  $\text{D}_2\text{O}$  ( $\text{H}_2\text{O}$ ), Fig. 3. These studies convincingly show that  $[\text{V}(\text{O})_2(\text{Hshed})]$  is destabilized by the RM environment more so than in aqueous solution. Slightly more  $[\text{V}(\text{O})_2(\text{Hshed})]$  complex was observed in larger RMs over smaller RMs.

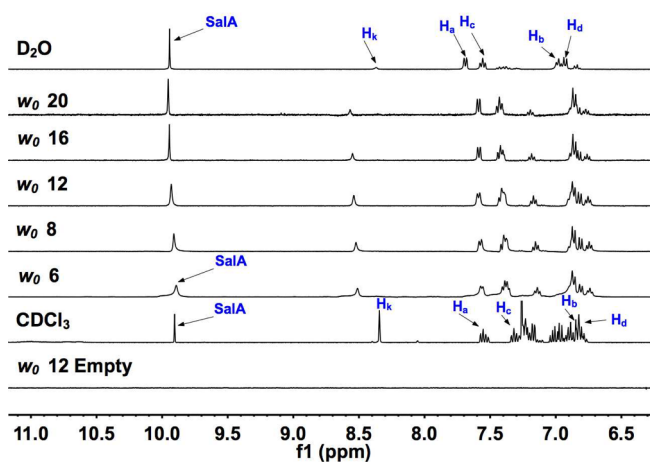


**Fig. 5**  $^1\text{H}$  NMR spectra of  $\text{H}_2\text{shed}$  in  $\text{D}_2\text{O}$  and in a series of RMs ( $w_0 = 6, 8, 12, 16,$  and  $20$  prepared from  $0.750 \text{ M}$  AOT/*iso*-octane stock solution. The spectrum in  $\text{D}_2\text{O}$  was recorded after 35 min and the spectra in RMs were recorded after 45 min once equilibrium had been established. Proton labelling scheme is found in Fig. 1. SalA = salicylaldehyde. The pH for  $\text{D}_2\text{O}$  and RMs was 6.6 and the pD was 7.0. The overall concentrations for the  $1.0 \text{ mL}$   $\text{H}_2\text{shed}$  RM samples are as follows:  $w_0 20, 2.71 \text{ mM}$ ;  $w_0 16, 5.65 \text{ mM}$ ;  $w_0 12, 11.77 \text{ mM}$ ;  $w_0 8, 24.48 \text{ mM}$ ; and  $w_0 6, 37.87 \text{ mM}$ .

**$^1\text{H}$  NMR Spectra of  $[\text{V}(\text{O})_2(\text{Hshed})]$  and  $\text{H}_2\text{shed}$ .** A series of  $^1\text{H}$  NMR spectroscopic studies in RMs were carried out using  $[\text{V}(\text{O})_2(\text{Hshed})]$ , and the corresponding free ligand,  $\text{H}_2\text{shed}$ . The RM studies with the  $[\text{V}(\text{O})_2(\text{Hshed})]$  complex confirmed that the free  $\text{H}_2\text{shed}$  ligand was formed from hydrolysis of complex which was then followed by subsequent hydrolysis of the  $\text{H}_2\text{shed}$  ligand to SalA and HyDA. The hydrolysis was confirmed in the  $\text{D}_2\text{O}$  spectra by the imine proton signal ( $\text{HC}=\text{N}$ ) at  $8.81 \text{ ppm}$  converting into an aldehyde proton ( $\text{HC}=\text{O}$ ) at  $9.98 \text{ ppm}$  (Fig. 4). These peaks are not present in the  $d_6$ -DMSO spectrum for  $[\text{V}(\text{O})_2(\text{Hshed})]$  (Fig. 4). The spectra are shown for RM sizes  $w_0 8$  through  $w_0 16$  and although the ligand hydrolysis is complete, increased reactions are taking place because increasing SalA:  $[\text{V}(\text{O})_2(\text{Hshed})]$  (the latter measured by  $\text{H}_k$ ) ratio is observed in the spectra as the RM size continues to increase (see spectrum at  $w_0 20$ ).

To further confirm the formation of the ligand hydrolysis product, SalA, a study of the non-complexed free ligand,  $\text{H}_2\text{shed}$ , in a series of RMs was carried out (Fig. 5). By monitoring the  $^1\text{H}$  NMR chemical shifts, it is apparent that the free ligand is hydrolyzing upon contact with the water pool (Fig. 5). Formation of an aldehyde group signal ( $\text{HC}=\text{O}$ ) at  $9.90 \text{ ppm}$  and a decrease in the imine signal ( $\text{HC}=\text{N}$ ) near  $8.5 \text{ ppm}$  readily shows the formation of one of the starting materials of the Schiff base, SalA and almost complete conversion is seen after an equilibrium time of 45 min in  $\text{D}_2\text{O}$ . The  $^1\text{H}$  NMR spectra demonstrated that the equilibrium mixture was different in the RMs compared to the  $\text{H}_2\text{shed}$  ligand in aqueous solution, and that the Schiff base is more stable in the environment of the smaller RMs in contrast to the  $[\text{V}(\text{O})_2(\text{Hshed})]$  complex. Combined, these results show that the SalA and the  $\text{H}_2\text{shed}$  begin to form both in solutions with uncomplexed free ligand

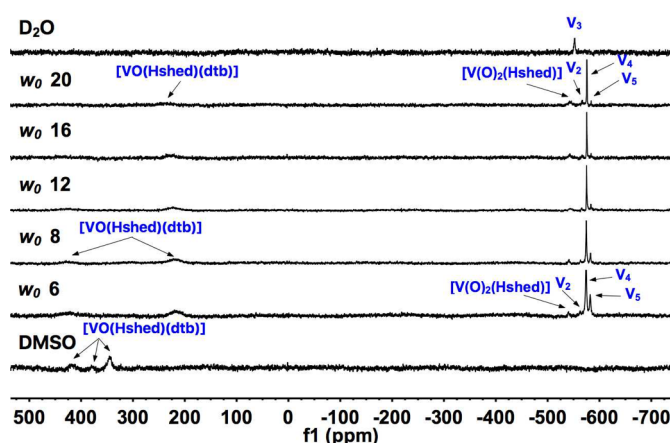


**Fig. 6**  $^{51}\text{V}$  NMR spectra of  $[\text{VO}(\text{Hshed})(\text{dtb})]$  in  $d_6$ -DMSO, *iso*-octane, and in a series of RMs ( $w_0 = 6, 8, 12, 16, 20$  prepared from 0.750 M AOT/*iso*-octane stock solution). The spectrum in  $\text{D}_2\text{O}$  was recorded after 60 min and the spectra in RMs was recorded after 50 min once equilibrium had been established. The pH for  $\text{D}_2\text{O}$  and RMs was 6.6 and the pD was 7.0. The total V-concentration for the 1.0 mL  $[\text{VO}(\text{Hshed})(\text{dtb})]$  RM samples are as follows:  $w_0$  20, 2.46 mM;  $w_0$  16, 5.23 mM;  $w_0$  12, 11.09 mM;  $w_0$  8, 23.55 mM;  $w_0$  6, 36.78 mM.

$\text{H}_2\text{shed}$  (Fig. 5) and with the precursor  $[\text{V}(\text{O})_2(\text{Hshed})]$  complex (Fig. 4).

There is a chemical shift change observed for  $[\text{V}(\text{O})_2(\text{Hshed})]$  protons  $\text{H}_a, \text{H}_b, \text{H}_c, \text{H}_d,$  and  $\text{H}_k$  upon addition to the RM, which showed a change in chemical environment and supported the interpretation that the  $[\text{V}(\text{O})_2(\text{Hshed})]$  complex penetrated at least partially into the RM interfacial layer (Fig. 4). The free ligand  $\text{H}_2\text{shed}$  hydrolyzed as evidenced by a peak at 9.94 ppm in  $\text{D}_2\text{O}$  and at 9.89 ppm in  $w_0$  8 RM (Fig. 4). There is a chemical shift change observed for  $\text{H}_2\text{shed}$  protons  $\text{H}_a, \text{H}_b, \text{H}_c, \text{H}_d,$  and  $\text{H}_k,$  which also showed a change in chemical environment and supported significant interaction of the  $\text{H}_2\text{shed}$  ligand with the RM interface (Fig. 5).

**NMR Spectra of  $[\text{VO}(\text{Hshed})(\text{dtb})]$  in Aqueous Solution and in RM Samples.**  $^{51}\text{V}$  NMR spectra were recorded to determine if the  $[\text{VO}(\text{Hshed})(\text{dtb})]$  complex hydrolyzed in aqueous solution and within RMs. This was non-trivial considering the low solubility of the complex in aqueous solution; therefore, these samples were prepared by dissolving the compound into the AOT/*iso*-octane stock solution rather than in the  $\text{D}_2\text{O}$  stock solution. The equilibrium for the hydrolysis products was observed in a saturated  $[\text{VO}(\text{Hshed})(\text{dtb})]/\text{D}_2\text{O}$  sample that was sonicated for 5 min, then vortexed for  $\sim 1$  min, and then allowed to sit for 60 min (Fig. 6).  $[\text{VO}(\text{Hshed})(\text{dtb})]$  hydrolyzed to form  $[\text{V}(\text{O})_2(\text{Hshed})]$  first and further hydrolysis formed vanadate and the  $\text{H}_2\text{shed}$  ligand according to eq. (3) and (4). The sample in  $d_6$ -DMSO (Fig. 6) contained three signals for  $[\text{VO}(\text{Hshed})(\text{dtb})]$ , the major peak signal is consistent with literature<sup>66</sup> and in addition we also observed two minor peaks, which we attribute to association and concentration phenomena. When placed in RMs, the equilibration was established slightly faster in this

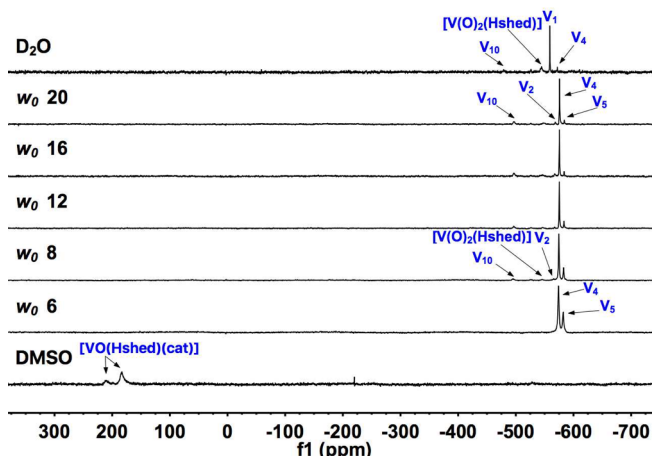
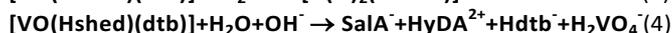


**Fig. 7**  $^{51}\text{V}$  NMR spectra of  $[\text{VO}(\text{Hshed})(\text{cat})]$  in  $\text{D}_2\text{O}$  and in a series of RMs ( $w_0 = 6, 8, 12, 16, 20$  prepared from 0.750 M AOT/*iso*octane stock solution). The spectra were recorded after equilibration was reached after 50 min for  $\text{D}_2\text{O}$  samples and after 40 min for RM samples. The pH for  $\text{D}_2\text{O}$  and RMs was 6.6 and the pD was 7.0. The total V-concentration for the 1.0 mL  $[\text{VO}(\text{Hshed})(\text{cat})]$  RM samples are as follows:  $w_0$  20, 2.41 mM;  $w_0$  16, 5.17 mM;  $w_0$  12, 11.05 mM;  $w_0$  8, 23.53 mM; and  $w_0$  6, 36.72 mM.

system ( $\sim 50$  min) after which time point the spectra no longer changed.

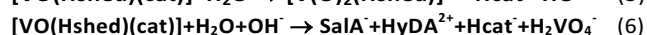
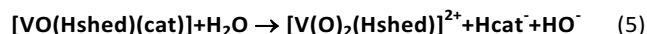


The NMR spectra recorded for  $[\text{VO}(\text{Hshed})(\text{dtb})]$  in  $d_6$ -DMSO,  $\text{D}_2\text{O}$ , and in RMs (RMs ( $w_0 = 6, 8, 12, 16,$  and  $20$ )) are shown in Fig. 6. The spectrum in  $d_6$ -DMSO shows three signals (see above). No complex is observed in the  $\text{D}_2\text{O}$  spectrum documenting that this compound is not soluble but does form vanadate and oligomers when attempting to dissolve the material. In the RM samples, more vanadate oligomers, possibly a little  $[\text{V}(\text{O})_2(\text{Hshed})]$ , and two signals, which are attributed to the  $[\text{VO}(\text{Hshed})(\text{dtb})]$  complex are observed (Fig. 6). Both  $^{51}\text{V}$  and  $^1\text{H}$  NMR spectra confirm that in RMs at higher concentration of the complex, more  $[\text{VO}(\text{Hshed})(\text{dtb})]$  is observed than in pure  $\text{D}_2\text{O}$ . When placing  $[\text{VO}(\text{Hshed})(\text{dtb})]$  in RMs, some of the complex hydrolyzed, and there was a large change in chemical shifts from the  $d_6$ -DMSO sample and the distribution of signals varied depending on the size of the RM. This suggests that the  $[\text{VO}(\text{Hshed})(\text{dtb})]$  complex is in an environment different from aqueous solution. As the size of the RM changed, the chemical shifts did not significantly change consistent with the possibility that the compound is in similar environments in the different sized RMs. These results are consistent with an interpretation that the  $[\text{VO}(\text{Hshed})(\text{dtb})]$  complex increases stability through association or interactions with the interface and although still separated from the water pool, the water reaches the complex, initiating hydrolysis of  $[\text{VO}(\text{Hshed})(\text{dtb})]$  and resulting in the formation of vanadate oligomers and  $[\text{V}(\text{O})_2(\text{Hshed})]$  (Fig. 6). As the RM size increases,

the amount of hydrolysis increases because the [VO(Hshed)(dtb)] complex signal decreases and the increase in oligomers formed is observed (as evidenced by the changes in the speciation).<sup>68</sup>

The <sup>1</sup>H NMR spectra of [VO(Hshed)(dtb)] in D<sub>2</sub>O, d<sub>6</sub>-DMSO, and various sized RMs were collected (see Supplementary Information Fig. S1). The spectrum in D<sub>2</sub>O does not show all the proton peaks present in the [VO(Hshed)(dtb)] complex due to limited solubility of the complex; however, the ligand of the complex was also hydrolyzed as evidenced by an aldehyde peak at 10.04 ppm in D<sub>2</sub>O and at 9.91 ppm in RMs. These peaks are not present in the d<sub>6</sub>-DMSO spectrum. There is a chemical shift change for [VO(Hshed)(dtb)] aromatic protons H<sub>b</sub>, H<sub>d</sub>, H<sub>e</sub>, and H<sub>f</sub>, which showed a change in environment of the complex and supports the interpretation based on the <sup>51</sup>V NMR spectra of an association and possible penetration of the complex into the RM interface. Combined, these studies show that the aqueous insoluble [VO(Hshed)(dtb)] complex can solubilize and partition in a heterogeneous environment, but such an environment also facilitates increased hydrolysis of the complex and its Schiff base ligand.

**NMR Spectra of [VO(Hshed)(cat)] in Aqueous Solution and in RM Samples.** <sup>51</sup>V NMR spectra were recorded as a function of time to determine if the [VO(Hshed)(cat)] complex hydrolyzed after it was dissolved in aqueous solution, as well as in AOT/*iso*-octane RMs (Fig. 7). The solubility of [VO(Hshed)(cat)] was limited in aqueous solution; therefore, ~1 min of vortexing was needed to prepare a saturated sample of [VO(Hshed)(cat)] in D<sub>2</sub>O. This system also had the potential of forming [V(O)<sub>2</sub>(Hshed)] and the H<sub>2</sub>shed ligand according to equations (5) and (6).



[VO(Hshed)(cat)] was dissolved in d<sub>6</sub>-DMSO and in aqueous solution as well as in AOT/*iso*-octane RMs. By <sup>51</sup>V NMR, no [VO(Hshed)(cat)] remained after being added to the D<sub>2</sub>O solution or the RM mixture and intact [VO(Hshed)(cat)] was only observed in d<sub>6</sub>-DMSO (Fig. 7). These results suggest that the equilibrium favors complex hydrolysis upon dissolution in D<sub>2</sub>O and that the energetics are not sufficiently favorable for the complex to reform in RM samples. <sup>1</sup>H NMR spectra shows that the H<sub>2</sub>shed ligand from the complex does hydrolyze more slowly, because some C=NH signal remains in w<sub>0</sub> 8-12 samples (see Fig. S2). These studies do confirm that the [VO(Hshed)(cat)] complex has significantly different properties than the [VO(Hshed)(dtb)] complex.

**Examining the AOT/*iso*-octane RMs Containing H<sub>2</sub>shed, [V(O)<sub>2</sub>(Hshed)], [VO(Hshed)(cat)] and [VO(Hshed)(dtb)] using Dynamic Light Scattering.** To determine if RMs formed in the AOT/RM samples, w<sub>0</sub> = 12 and w<sub>0</sub> = 20 RM samples were investigated using Dynamic Light Scattering (DLS). In Table S1 the RM samples are listed with the no cargo, with H<sub>2</sub>shed, with [V(O)<sub>2</sub>(Hshed)], with [VO(Hshed)(cat)] or with [VO(Hshed)(dtb)].

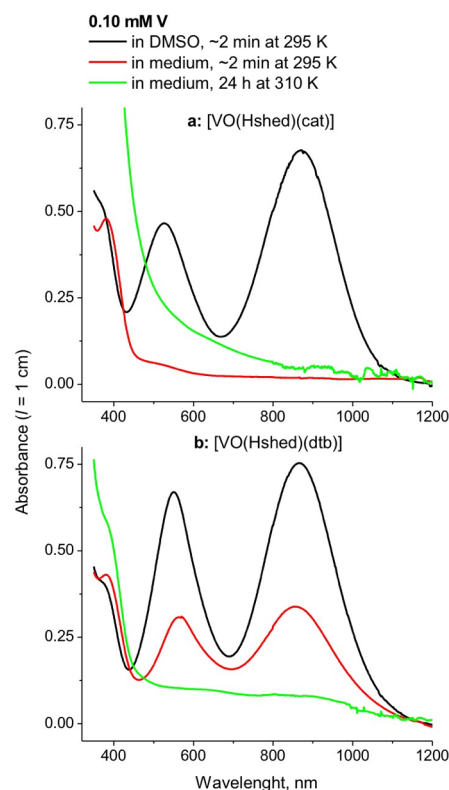


**Fig. 8** Representative absorption spectra of fresh (2 min after dissolution) and aged (24 h after dissolution) of (a) [VO(Hshed)(cat)] and (b) [VO(Hshed)(dtb)] (0.10 mM V-compound) in DMSO solutions or in cell culture medium (Advanced DMEM, containing 2.0% vol. of fetal calf serum and 10 mM HEPES buffer, pH 7.4).

The results show that AOT/*iso*-octane RM structures form in all cases and that the sizes are comparative with literature values.<sup>69</sup> Furthermore, there were no significant differences observed between the hydrodynamic radii of the empty RM samples and those containing cargo. This suggests that no significant changes in the structures of the RMs are induced upon placement of any of the probe molecules inside the RMs.

**The Anticancer Effects of V(V) Catecholate Complexes on Bone Cancer Cells (SW1353 cells).** The hydrophobicity of the [VO(Hshed)(dtb)] complex enhances complex stability to hydrolysis and thus increases the ability of the compound to enter cells intact. The question whether increased uptake due to hydrophobicity will be reflected in increased cytotoxicity was investigated in human chondrosarcoma cells, SW1353. However, before these studies were carried out we determined the stability of the compounds in cell culture media (Advanced DMEM, supplemented with 2.0% vol. of fetal calf serum and 10 mM of HEPES buffer to maintain pH = 7.4 under ambient atmosphere)<sup>30</sup> using absorption spectroscopy, because both [VO(Hshed)(cat)] and [VO(Hshed)(dtb)] showed strong absorbance bands in the visible and near-IR range in accord with literature.<sup>66</sup>

As shown in Fig. 8, the absorption spectra of the [VO(Hshed)(dtb)] complex show intact complex in DMSO and fresh media (DMSO shown with black lines in Fig. 8; fresh media are red). Although the complex is intact in DMSO, the [VO(Hshed)(dtb)] complex is only partially stable over time in cell media where it ultimately undergoes hydrolysis. However, after 24 h the [VO(Hshed)(dtb)] complex had degraded (shown with green lines in Fig. 8). In contrast, addition of [VO(Hshed)(cat)] (0.10 mM V-complex) to cell culture medium instantly caused disappearance of the characteristic absorbance bands of the complex at  $\sim 530$  nm and  $\sim 870$  nm (red line in Fig. 8a). The [VO(Hshed)(cat)] complex is therefore much less stable than the [VO(Hshed)(dtb)] complex. These results are consistent with the results by NMR spectroscopic studies described above (Fig. 6 and 7). Both complexes decomposed after 24 h incubation with the cell culture medium at 310 K. The following cell culture studies were therefore done with both fresh and aged solutions. This allowed us to compare the effects over time for the two different V(V) Schiff base/catecholate compounds and vanadate in bone cancer cells (human chondrosarcoma, SW1353 cells). This also permitted us to explore when [VO(Hshed)(dtb)] was still intact and when both complexes were hydrolysed.

Initial experiments on the anti-proliferative activities of the [VO(Hshed)(cat)] and [VO(Hshed)(dtb)] complexes in SW1353 cells (Fig. 9a) were carried out with the consideration of their different hydrolysis rates in aqueous solutions, in cell culture media and in artificial membrane systems (Fig. 6-9). Stock solutions of both complexes in DMSO, which were stable for at least 24 h under ambient conditions (verified by electronic absorption spectroscopy, Fig. 8) were added to cell culture medium to the required final concentrations (typically,  $5.0 \mu\text{M}$  V). The resultant medium was either immediately added to the cells (within 1 min fresh medium), or allowed to age for 24 h ( $310 \text{ K}$ ,  $5\% \text{ CO}_2$ ) prior to addition to the cells.<sup>70</sup> Vanadate ( $\text{Na}_3\text{VO}_4$ , either fresh or aged in the medium) was used as a reference compound.<sup>32</sup> Previous studies by XANES spectroscopy<sup>35</sup> and EPR spectroscopy<sup>71</sup> have shown that vanadate converts to a mixture of V(V) (predominantly) and V(IV) complexes with medium components upon aging. As shown in Fig. 9a, [VO(Hshed)(cat)] was moderately active at  $5.0 \mu\text{M}$  V-complex (cell viability after 72 h treatment was 40-50% of control), while  $\text{Na}_3\text{VO}_4$  added to the media resulted in 70-75% of the control. For [VO(Hshed)(cat)] and vanadate, no significant difference in anti-proliferative activity was observed between fresh and aged solutions in cell culture medium.

The [VO(Hshed)(dtb)] complex showed much stronger anti-proliferative activity when freshly added to the medium (only  $\sim 2\%$  of control), compared with the aged solution (50-60% of control) (Fig. 9a). Furthermore, compared to the less hydrophobic [VO(Hshed)(cat)] complex or the ionic vanadate, the fresh solution of the more hydrophobic and intact [VO(Hshed)(dtb)] complex was significantly more potent. As a result, we were interested in exploring the anti-proliferative activity of [VO(Hshed)(dtb)] further. Concentration-dependent studies of fresh [VO(Hshed)(dtb)] solutions using two different assays for cell viability, WST-8<sup>72</sup> and Alamar Blue,<sup>73</sup> gave

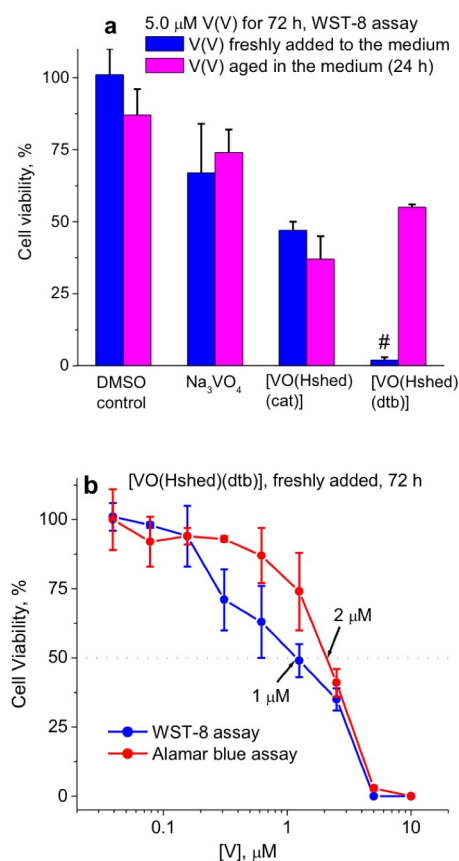


**Fig. 9** Anti-proliferative activity of [VO(Hshed)(cat)], [VO(Hshed)(dtb)] and  $\text{Na}_3\text{VO}_4$  in human chondrosarcoma (SW1353) cells: (a) comparative effects of V(V) complexes at  $5.0 \mu\text{M}$  V; and (b) concentration-dependent effects for fresh solutions of [VO(Hshed)(dtb)]. Treatment media were added to cells either within 1 min after the addition of V(V) complexes (fresh media), or pre-incubated with the V(V) complexes for 24 h at  $310 \text{ K}$  and  $5\% \text{ CO}_2$  before the addition to cells (aged media). In both cases, cells were treated for 72 h ( $310 \text{ K}$ ,  $5\% \text{ CO}_2$ ) before the determination of cell viability by endpoint colorimetric assays (WST-8 or Alamar Blue). All the treatments, including controls, contained  $0.50\%$  vol. DMSO. Error bars represent the mean values and standard deviations of six replicate wells. The # sign shows highly significant difference ( $P < 0.001$ ) in activity between fresh and decomposed solutions of [VO(Hshed)(dtb)].

consistent results with  $IC_{50} = 1.3 \pm 0.3 \mu\text{M}$  V and a plateau is seen at high V-concentrations ( $5\text{-}10 \mu\text{M}$ ) (Fig. 9b). This level of activity is similar or higher compared to that of well-established Pt(II) anti-cancer drugs in typical human cancer cell lines ( $IC_{50} \sim 1\text{-}5 \mu\text{M}$  Pt)<sup>74</sup>. Taken together, data from Fig. 6-8 shows that higher stability of [VO(Hshed)(dtb)] compared with [VO(Hshed)(cat)] in cell culture medium and in the hydrophobic environment of cell membranes is likely to lead to its significant cellular uptake before hydrolysis in aqueous medium is complete.<sup>75</sup> The observed higher cytotoxicity of fresh solutions in cell culture medium compared to aged ones correlates with the greater stability of the [VO(Hshed)(dtb)] complex. High hydrolysis rates of [VO(Hshed)(cat)] in cell culture medium (Fig.

8) are likely to prevent cellular uptake of the intact complex, which means that the anti-proliferative activity is due to decomposition products as have been recognized previously in multiple biological systems.<sup>4, 10, 32, 76-83</sup> Similar relation between aqueous stability, cellular uptake and anti-proliferative activity was observed previously for Ru complexes.<sup>84, 85</sup> We conclude that the increased hydrophobicity of the dtb catechol ligand is preventing early hydrolysis leading to the enhanced cellular uptake of intact [VO(Hshed)(dtb)] complex.

**Discussion.** Numerous studies were carried out with different V compounds exploring the mode of action and the identity of the active species when V-compounds were considered for treatment of diabetes.<sup>4, 56, 80, 86, 87</sup> It is well-known that V-compounds are protein tyrosine phosphatase inhibitors,<sup>56, 88, 89</sup> however, much work has been done on the transport of V-compounds from the administration site to the site of action.<sup>39, 90-92</sup> Specifically, studies have been done exploring the transport of V-compounds in blood,<sup>37, 38, 91, 93, 94</sup> and the speciation of these compounds<sup>13, 56, 95</sup> have been investigated in detail both in model systems,<sup>38, 94</sup> in blood,<sup>37, 91, 93</sup> in animal model studies<sup>96</sup> and in human studies.<sup>11</sup> Interaction of V-compounds with transferrin, human serum albumin or other blood components have demonstrated that V-compounds can lose one or more of their ligands and remain active.<sup>37, 91, 93, 97</sup> How the vanadium compounds and what properties dictate entrance into the cells remains an important question.

These studies have shown that the interface dramatically impacted the stability of the vanadium precursor complex, [V(O)<sub>2</sub>(Hshed)], as well as two hydrophobic vanadium complexes, [VO(Hshed)(cat)] and [VO(Hshed)(dtb)]. Both ternary mixed-ligand complexes are soluble in the polar organic solvents such as DMSO and less so in nonpolar organic solvents (e.g., 2,2,4-trimethylpentane). However, the inhomogeneous environment of a microemulsion supports these complexes even if they have been hydrolyzed in the presence of interfacial water. Based on the NMR spectroscopic studies presented in this work, the interaction with the RM interface protects the V-compound against rapid initial hydrolysis. The slowed hydrolysis effect was more pronounced for the more sterically-hindered hydrophobic dtb ligand. This effect could be due to sterics or hydrophobicity of the ligand or a combination of both and studies with additional compounds will shed light as to the origin of this observation. Alternatively, it may be possible that pKa values of the catechols can affect the inherent thermodynamic stability of the coordination complexes. The pKa value of the parent catechol is higher than that of the t-butyl substituted catechol and thus, the coordinated complex of the latter would be more stable. Initial V-complex stability may be important for the anti-cancer activity of the compounds as shown by the study in human bone cancer cells (chondrosarcoma) and the anti-cancer effects trace with the hydrophobicity, decreased hydrolytic stability, or increased thermodynamic stability of the V-compounds. Future studies with additional related V-compounds will shed further light on the exact origin of the anticancer effects.

The kinetic stability of [VO(Hshed)(dtb)] in water and aqueous media is unusual for a V-complex but in this case, provides sufficient stability to enable this complex to enter cancer cells intact. The hydrophobic environment of the cell membrane is likely to further stabilize this compound.<sup>40</sup> This unusual short-term stability of this highly cytotoxic complex may show considerable promise in cancer treatment, particularly against aggressive cancers such as prostate cancer. Since such hydrophobic complexes are likely to undergo cellular uptake via passive diffusion through the cell membrane, it is important to investigate if hydrophobicity or hydrolytic stability of these compounds correlates with uptake in membrane model systems.

The results presented here with two different hydrophobic catecholate complexes based on studies in AOT-*iso*-octane microemulsion system shows that although the [VO(Hshed)(dtb)] complex may be stabilized; the membrane system is not able to completely prevent hydrolysis from the water penetrating the interface. If a complex remains intact for some limited time, this will allow the drug to reach the cellular target intact. Importantly, the current results show that the intact complexes indeed interact with the interface and, hence, the results are consistent with the observation of increased cytotoxicity of fresh versus aged drug preparation. That is, the freshly prepared solution contains more intact complex and the hydrolyzed aged solution contains less intact complex. Accordingly, the solution with more intact [VO(Hshed)(dtb)] complex is much more cytotoxic compared to the aged solution with degraded V-complex towards the bone cancer cells investigated. Importantly, the results with the aged solutions shows dramatically decreased cytotoxic effect for both V-complexes against SW153 bone cancer cells, consistent with the free ligands having no significantly cytotoxicity (free ligands alone are significantly less cytotoxic (unpublished data)).

Given the fact that humans are largely composed of water and cell assay studies generally are done using water-based approaches, administration of hydrophobic drugs remains a challenge. However, there are ways of delivering a drug into the body that does not require water solubility but in the case of these very hydrophobic drugs, cell assays in aqueous solution remains problematic. The studies described herein may imply that hydrophobic metallo-compounds with increased hydrolytic stability will continue to be of interest and suggests that alternative approaches for effective drug delivery that will circumvent significant decomposition should be developed.

## Conclusions

The [VO(Hshed)(cat)] complex is found to have lower thermodynamic stabilities in both water and cell culture medium compared to the [VO(Hshed)(dtb)] complex. Although the complexes show limited stability in the presence of membrane model systems, this may be a consequence of the pre-equilibrium that resulted in partial hydrolyzed complex(es). The greater activities observed in fresh solutions of V-catecholate complexes containing higher amounts of intact compound in *in vitro* cytotoxicity assays in bone cancer cells and

are in line with additional studies in MDA-MB-231 and PANC-1 cells.<sup>40</sup> Importantly, the membrane model results shown here demonstrate that the intact V(V) catecholates will penetrate the membrane, which supports the cell cytotoxicity assays that indicate the intact complexes are taken up before they are decomposed in the cell medium.

In summary, the hydrophobic V(V) catecholates compounds presented here are found to interact with membrane model systems and the V-complex with the highest stability is found to have the most potent anti-cancer properties. It is possible that complexes containing hydrophobic ligands with sterically hindered V-atom preventing substitution reactions may enable uptake of the intact complex and delivery to the cellular target. Alternatively, similar behavior could arise from different thermodynamic stabilities. Regardless of the origin, the hydrophobic V(V) catecholates complexes were found to be a particularly potent cytotoxin to bone cancer cells. These results warrant future studies of such and similarly stable hydrophobic vanadium compounds as potential anti-cancer agents.

## Experimental section

**Chemicals, Biochemicals, and General Methods.** Most reagents were used without further purification including 2,2,4-trimethylpentane (*iso*-octane, Sigma-Aldrich, ≥99.0%), deuterium oxide (D<sub>2</sub>O, Cambridge Isotope Laboratories, 99.9%), Acetone HPLC grade, *n*-pentane, and argon. Sodium bis(2-ethylhexyl)sulfosuccinate (AOT, Sigma-Aldrich, 99.8%) was purified using activated charcoal and methanol to remove acidic impurities using a modified procedure of that previously reported (see below).<sup>10, 98, 99</sup> Salicylaldehyde (SaA) was purified via vacuum distillation to remove impurities prior to synthesis. [V(O)<sub>2</sub>(Hshed)], H<sub>2</sub>shed, [VO(Hshed)(cat)], and [VO(Hshed)(dtb)] were prepared according to literature procedures.<sup>65-67</sup> All pH measurements were conducted using a Thermo Orion 2 Star pH meter with a VWR semi-micro pH probe.<sup>86</sup> When samples were prepared for RM or D<sub>2</sub>O NMR experiments, deuterium oxide was used instead of H<sub>2</sub>O and the pH was adjusted to consider the presence of deuterium (pD = pH + 0.4) and therefore we report values for both pD and pH for clarity.<sup>99, 100</sup> Pre-sterilized media and sterile plastic ware used in cell culture were purchased from Life Technologies Australia. Human chondrosarcoma SW1353 cells were purchased from the American Type Culture Collection (ATCC, Cat. No. HTB-94) and cultured using standard techniques.<sup>101, 102</sup> in Advanced DMEM (where DMEM = Dulbecco's modified Eagle's medium; Thermo Fischer Scientific, Cat. No. 12491-015). Abbreviations are as follows: aot, bis(2-ethylhexyl) sulfosuccinate sodium salt; cat, catecholate; dtb, di-*tert*-butylcatecholate; DLS, dynamic light scattering; HEPES, (4-(2-hydroxyethyl)-1-piperazine-ethanesulfonic acid; H<sub>2</sub>shed, condensation product of salicylaldehyde and *N*-(2-hydroxyethyl)-1,2-ethanediamine; pdi, polydispersity index; SaA, salicylaldehyde; HyDA, ethanediamine; CCR2, CC chemokine receptor 2; CCL2, CC chemokine ligand 2; CCR5, CC chemokine receptor 5; TLC, thin layer chromatography.

**Purification of NaAOT.** NaAOT was purified by a slightly modified procedure from that reported previously.<sup>43, 103</sup> AOT (60.0 g) was dissolved in methanol (150 mL) and the solution was shaken for a period of two weeks in the presence of mesh activated charcoal (15.0 g).<sup>43, 103</sup> The suspension was then vacuum filtered through a bed of celite and then the methanol was removed, first via rotary evaporation under reduced pressure at room temperature and then

via high vacuum (~150 milli Torr) until desired dryness was achieved. The residual water content ranged from 0.019 to 0.300 waters per AOT and was measured as previously reported.<sup>41</sup>

### Preparation of AOT/*iso*-octane Stock Solution and RMs Samples.

The 750 mM AOT/*iso*-octane stock solution was prepared by dissolving AOT (8.333 g, 18.80 mmol) in *iso*-octane in a volumetric flask (25.00 mL), diluting to the mark, and vortexing until clear. For all six probe molecules studied, a 52.75 mM stock solution was used to prepare RM containing suspensions. The stock solution was prepared by dissolving the probe molecule (0.5275 mmol) in 750 mM AOT/*iso*-octane stock in a volumetric flask (10.00 mL), diluting to the mark, and mixing until solubilized. The probe AOT/*iso*-octane stock solutions containing either vanadium or the H<sub>2</sub>shed ligand were mixed by hand and not vortexed to have as little outside impact on hydrolysis as possible. Before the preparation of the 1 mL RM samples, 2 mL solutions of varying concentrations of probe stock were created by diluting various aliquots of the 52.75 mM probe stock with the 750 mM AOT/*iso*-octane stock. Then, the 1 mL RM samples ( $w_0 = 6, 8, 12, 16, \text{ and } 20$ ) were made by diluting specific aliquots of the 2 mL solutions with various amounts of D<sub>2</sub>O (pH = 6.6, pD = 7.0, see General Methods for pH measurements). The addition of the D<sub>2</sub>O resulted in the formation of a white flocculent at the bottom of the samples and, when shaken, a homogenous solution resulted. For the free H<sub>2</sub>cat and H<sub>2</sub>dtb ligand RM samples, NMR studies were done immediately after preparation while the free H<sub>2</sub>shed ligand, [V(O)<sub>2</sub>(Hshed)], [VO(Hshed)dtb], and [VO(Hshed)cat] RM samples were allowed to equilibrate before the NMR spectroscopic studies were performed. The total V-concentration for the 1.0 mL [V(O)<sub>2</sub>(Hshed)] RM samples are as follows:  $w_0$  20, 2.41 mM;  $w_0$  16, 5.17 mM;  $w_0$  12, 11.05 mM;  $w_0$  8, 23.53 mM; and  $w_0$  6, 36.72 mM. The overall concentrations for the 1.0 mL H<sub>2</sub>shed RM samples are as follows:  $w_0$  20, 2.71 mM;  $w_0$  16, 5.65 mM;  $w_0$  12, 11.77 mM;  $w_0$  8, 24.48 mM; and  $w_0$  6, 37.87 mM. The total V-concentration for the 1.0 mL [VO(Hshed)(dtb)] RM samples are as follows:  $w_0$  20, 2.46 mM;  $w_0$  16, 5.23 mM;  $w_0$  12, 11.09 mM;  $w_0$  8, 23.55 mM;  $w_0$  6, 36.78 mM. The total V-concentration for the 1.0 mL [VO(Hshed)(cat)] RM samples are as follows:  $w_0$  20, 2.41 mM;  $w_0$  16, 5.17 mM;  $w_0$  12, 11.05 mM;  $w_0$  8, 23.53 mM;  $w_0$  6, 36.72 mM.

**Stability of Probe in Aqueous Solution and RMs.** The stability of the precursor complex [V(O)<sub>2</sub>(Hshed)], vanadium(V) catecholates [VO(Hshed)dtb] and [VO(Hshed)cat], and the free ligand H<sub>2</sub>shed in aqueous solution was determined by solution NMR spectroscopy. NMR measurements of the hydrolysis of each probe molecule in D<sub>2</sub>O (pH = 6.6, pD = 7.0, see General Methods for pH measurements) were done until the probe molecule had reached equilibrium as evidenced by the NMR peak integrations changing over time. Similar equilibrium stability measurements were taken for each V-compound in a  $w_0 = 12$  RM. Once the equilibrium had been determined for each probe molecule in a RM system, complete RM studies were performed at the determined equilibrium time point.

**<sup>1</sup>H and <sup>51</sup>V NMR Spectroscopic Studies on RM Samples.** All <sup>51</sup>V solution NMR spectra were taken on a Varian 400MR NMR spectrometer with a spectral window of -700 ppm to 700 ppm, 4096 scans, RD = 0.001 sec, and 90° pulse angle at 26 °C. The <sup>1</sup>H NMR spectroscopic experiments on the RMs were performed using a 400 MHz Varian iNova NMR spectrometer or a 400 MHz MR400 spectrometer, using standard parameters at 22 or 26 °C, respectively. The 1D <sup>1</sup>H spectra in CDCl<sub>3</sub> or d<sub>6</sub>-DMSO were referenced to the internal solvent peak at 7.26 ppm and 2.50 ppm, respectively.

## ARTICLE

## Dalton Transactions

The  $1D^1H$  spectra in RMs were referenced to the *iso*-octane methyl peak (0.904 ppm) as previously reported.<sup>99</sup>  $^{51}V$  solution chemical shifts in DMSO are determined relative to external neat liquid  $VOCl_3$  reference (0.00 ppm).<sup>104</sup>  $^{51}V$  solution chemical shifts in  $D_2O$  or RMs are measured relative to an external 1 M sodium metavanadate reference (pH = 12) which, in aqueous solution, produces two signals at -535.7 ppm (used as auxiliary reference) and -560.4 ppm, relative to  $VOCl_3$ .<sup>105</sup> Spectral data was processed using MestReNova NMR processing software version 10.0.1.

#### RM Sample Preparation for Dynamic Light Scattering (DLS) Studies.

RMs for DLS studies were prepared in a similar manner to those used for the NMR spectroscopic experiments except that Distilled Deionized (DDI)  $H_2O$  (pH = 6.6) was used as the water pool instead of  $D_2O$ , and the 0.750 M AOT/RM solution was diluted to a 0.1 M AOT/RM solution with *iso*-octane after the RMs were formed.

**DLS Measurements.** The hydrodynamic radius of  $w_0 = 12$  and  $w_0 = 20$  RMs was determined by DLS measurements performed on a Malvern Zetasizer Nano ZS instrument (Malvern Instruments, Malvern, UK). The DLS cuvette (1 cm X 1 cm, glass) was washed three times with *iso*-octane followed by three washes with the RM sample (prepared at pH 6.6). Then, the cuvette was filled with 1 mL of the RM sample and closed with a Teflon cap. Each experiment was conducted at 25 °C and consisted of a 700 sec. sample equilibration period followed by 10 measurements each made of 15 scans.<sup>106</sup> Each sample was measured in triplicate, and the diameter and pdi were recorded and compared to those values in the literature.<sup>69</sup> The data were analyzed using Malvern DLS Software. See Supplementary Information.

**Stability Studies by Electronic Absorption Spectroscopy.** Freshly prepared stock solutions of [VO(Hshed)(cat)] or [VO(Hshed)(dtbc)] (10 mM V-complex in DMSO) were diluted 100-fold either with DMSO or with cell culture medium (Advanced DMEM, containing 2.0% vol. of fetal calf serum and 10 mM HEPES buffer, pH 7.4)<sup>30</sup>. The spectra in the 350-1200 nm range (resolution, 1 nm; acquisition rate, 600 nm min<sup>-1</sup>) were acquired on an Agilent Cary 5000 spectrometer at 295 K. The corresponding solvents were used in background scans.

**Cytotoxicity Experiments.** Advanced DMEM medium (Thermo Fisher Scientific Cat. No. 12491-015, where DMEM = Dulbecco's modified Eagle's medium) was supplemented with L-glutamine (2.0 mM), antibiotic-antimycotic mixture (100 U mL<sup>-1</sup> penicillin, 100 mg mL<sup>-1</sup> streptomycin and 0.25 mg mL<sup>-1</sup> amphotericin B) and fetal calf serum (FCS; heat-inactivated; 2% vol.). For proliferation experiments, cells were seeded in 96-well plates at an initial density of  $1.0 \times 10^3$  viable cells per well (counted using Invitrogen Countess device with trypan blue staining)<sup>101, 102</sup> in 100  $\mu$ L medium and left to attach overnight. Freshly prepared 10 mM stock solutions in DMSO ([VO(Hshed)(dtb)] or [VO(Hshed)(cat)]) or in Milli-Q  $H_2O$  ( $Na_3VO_4$ , 99.98%, Aldrich Cat. No. 450243) were used for cell assays. All the cell treatments, including controls, contained 0.50% (vol.) of DMSO.<sup>107</sup> Stock solutions of the treatment compounds were diluted with fully supplemented cell culture media to the required final concentrations, and the resultant media were either added to the cells within one minute (fresh solutions) or left in cell culture incubator (310 K, 5%  $CO_2$ ) for 24 prior to the cell treatments (aged solutions). For end-point viability assays, cells were incubated with fresh or aged treatment compounds for 72 h, after which WST-8 reagent (Cell counting kit-8, Dojindo Molecular Technologies) or Alamar Blue reagent (Thermo Fisher Scientific Cat. No. DAL1025) was added at 10  $\mu$ L/well. The cells were then incubated for further six

hours, and the absorbance at 450 nm (WST-8) or fluorescence at 570/585 nm (Alamar Blue) were measured using Victor V<sup>3</sup> multi-well plate reader. For each treatment, six replicate cell-containing wells and two background wells (containing all the components except cells) were used, and statistical analysis of the data was performed using Origin software.<sup>108</sup> Preliminary calibration experiments with WST-8 assay have shown that the  $A_{450}$  values in the entire working range (0.25-1.5) were linearly dependent on the number of viable SW1353 cells ( $\sim 10^2$ - $10^4$  cells per well).

#### Conflicts of interest

There are no conflicts to declare.

#### Acknowledgements

DCC and PAL thank the University of Sydney for an International Scholar Award to DCC. SMP and DCC thank the NSF REU (CHE-1461040) for summer support to SMP. DCC also thanks the Arthur Cope Foundation Administered by the American Chemical Society for partial support. Financial support for this work was also provided by Australian Research Council (ARC) grants to PAL including support for an ARC Senior Research Associate position to AL (DP130103566, DP160104172).

#### References

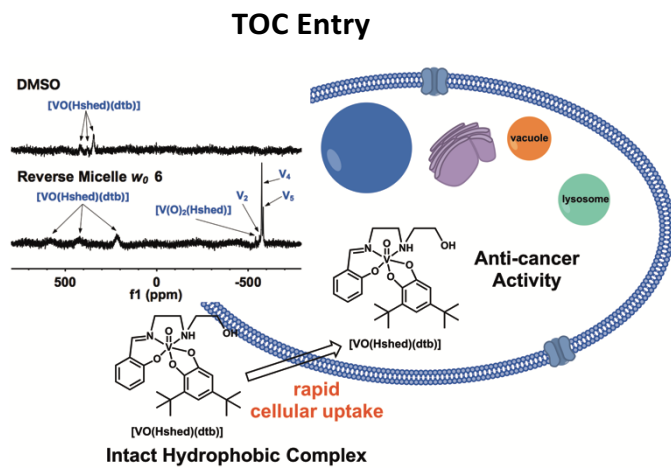
1. S. E. Sherman and S. J. Lippard, *Chem. Rev.*, 1987, **87**, 1153-1181.
2. A. M. Evangelou, *Crit. Rev. Oncol. Hematol.*, 2002, **42**, 249-265.
3. N. Farrell, *Met. Ions Biol. Syst.*, 1996, **32**, 603-639.
4. J. C. Pessoa, S. Etcheverry and D. Gambino, *Coord. Chem. Rev.*, 2015, **301**, 24-48.
5. X. Yang and K. Wang, *Curr. Top. Med. Chem.*, 2016, **16**, 675-676.
6. S. Petanidis, E. Kioseoglou, K. Domvri, P. Zarogoulidis, J. M. Carthy, D. Anastakis, A. Moustakas and A. Salifoglou, *Int. J. Biochem. Cell Biol.*, 2016, **74**, 121-134.
7. A. P. Vieira, C. A. Wegemann and A. M. Da Costa Ferreira, *New J. Chem.*, 2018, **42**, 13169-13179.
8. K. Gruzewska, A. Michno, T. Pawelczyk and H. Bielarczyk, *J. Physiol. Pharmacol.*, 2014, **65**, 603-611.
9. D. Rehder, J. C. Pessoa, C. Geraldes, M. Castro, T. Kabanos, T. Kiss, B. Meier, G. Micera, L. Pettersson, M. Rangel, A. Salifoglou, I. Turel and D. R. Wang, *J. Biol. Inorg. Chem.*, 2002, **7**, 384-396.
10. K. H. Thompson, J. Lichter, C. LeBel, M. C. Scaife, J. H. McNeill and C. Orvig, *J. Inorg. Biochem.*, 2009, **103**, 554-558.
11. G. R. Willsky, K. Halvorsen, M. E. Godzala, III, L.-H. Chi, M. J. Most, P. Kaszynski, D. C. Crans, A. B. Goldfine and P. J. Kostyniak, *Metallomics: integrated biometal science*, 2013, **5**, 1491-1502.
12. D. C. Crans, L. Yang, A. A. Haase and X. Yang, *Met. Ions Life Sci.*, 2017, **18**, 251-280.
13. D. C. Crans, K. A. Woll, K. Prusinskas, M. D. Johnson and E. Norkus, *Inorg. Chem.*, 2013, **52**, 12262-12275.
14. C. A. Lipinski, F. Lombardo, B. W. Dominy and P. J. Freaney, *Adv. Drug Delivery Rev.*, 2001, **46**, 3-26.
15. P. Köpf-Maier, *Met. Complexes Cancer Chemother.*, 1993, 259-296.
16. P. Ghosh, O. J. D'Cruz, R. K. Narla and F. M. Uckun, *Clin. Cancer Res.*, 2000, **6**, 1536-1545.
17. I. Kostova, *Anti-Cancer Agents Med. Chem.*, 2009, **9**, 827-842.
18. I. León, N. Butenko, A. Di Virgilio, C. Muglia, E. Baran, I. Cavaco and S. Etcheverry, *J. Inorg. Biochem.*, 2014, **134**, 106-117.
19. I. León, J. Cadavid-Vargas, A. Di Virgilio and S. Etcheverry, *Curr. Med. Chem.*, 2017, **24**, 112-148.
20. B. I. Posner, A. Shaver and I. G. Fantus, in *New Antidiabetic Drugs*, eds. C. J. Bailey and P. R. Flatt, Smith-Gordon, London, 1990, vol. Chapter 8, pp. 107-118.
21. M. Li, W. Ding, B. Baruah, D. C. Crans and R. Wang, *J. Inorg. Biochem.*, 2008, **102**, 1846-1853.
22. L. P. Lu and M. L. Zhu, *Anti-Cancer Agents Med. Chem.*, 2011, **11**, 164-171.

23. D. C. Crans, M. L. Tarlton and C. C. McLauchlan, *Eur. J. Inorg. Chem.*, 2014, 4450-4468.
24. C. C. McLauchlan, B. J. Peters, G. R. Willsky and D. C. Crans, *Coord. Chem. Rev.*, 2015, **301-302**, 163-199.
25. L. Reytmán, O. Braitbard, J. Hochman and E. Y. Tshuva, *Inorg. Chem.*, 2016, **55**, 610-618.
26. H. Glasner, S. Meker and E. Y. Tshuva, *J. Organomet. Chem.*, 2015, **788**, 33-35.
27. S. Clede, F. Lambert, R. Saint-Fort, M.-A. Plamont, H. Bertrand, A. Vessieres and C. Policar, *Chem. Eur. J.*, 2014, **20**, 8714-8722.
28. P. Khosravi-Shahi, L. Cabezón-Gutiérrez and S. Custodio-Cabello, *Asia-Pac. J. Clin. Oncol.*, 2018, **14**, 32-39.
29. I. Correia, L. Chorna, I. Cavaco, S. Roy, M. L. Kuznetsov, N. Ribeiro, G. Justino, F. Marques, T. Santos-Silva, M. F. A. Santos, H. M. Santos, J. L. Capelo, J. Douth and J. C. Pessoa, *Chem. Asian J.*, 2017, **12**, 2062.
30. A. Levina, D. C. Crans and P. A. Lay, *Coord. Chem. Rev.*, 2017, **325**, 473-498.
31. A. Levina and P. A. Lay, *Dalton Trans.*, 2011, **40**, 11675-11686.
32. A. Levina and P. A. Lay, *Chem. Asian J.*, 2017, **12**, 1692-1699.
33. M. Le, O. Rathje, A. Levina and P. A. Lay, *J. Biol. Inorg. Chem.*, 2017, **22**, 663-672.
34. A. Levina, A. I. McCloud, S. J. Gasparini, A. Nguyen, W. G. M. De Silva, J. B. Aitken, H. H. Harris, C. Glover, B. Johannessen and P. A. Lay, *Inorg. Chem.*, 2015, **54**, 7753-7766.
35. A. Levina, A. I. McCloud, A. Pulte, J. B. Aitken and P. A. Lay, *Inorg. Chem.*, 2015, **54**, 6707-6718.
36. D. Sanna, V. Ugone, M. Serra and E. Garrriba, *J. Inorg. Biochem.*, 2017, **173**, 52-65.
37. D. Sanna, V. Ugone, G. Micera, P. Buglyo, L. Biro and E. Garrriba, *Dalton Trans.*, 2017, **46**, 8950-8967.
38. D. Sanna, G. Micera and E. Garrriba, *Inorg. Chem.*, 2013, **52**, 11975-11985.
39. D. Sanna, V. Ugone, G. Sciortino, P. Buglyo, Z. Bihari, P. L. Parajdi-Losoncz and E. Garrriba, *Dalton Trans.*, 2018, **47**, 2164-2182.
40. A. Levina, A. Wijetunga, R. Kaur, J. T. KoeHN, D. C. Crans and P. A. Lay, *To Be Submitted*.
41. M. L. Stahla, B. Baruah, D. M. James, M. D. Johnson, N. E. Levinger and D. C. Crans, *Langmuir*, 2008, **24**, 6027-6035.
42. D. C. Crans, C. D. Rithner, B. Baruah, B. L. Gourley and N. E. Levinger, *J. Am. Chem. Soc.*, 2006, **128**, 4437-4445.
43. J. Eastoe, B. H. Robinson and R. K. Heenan, *Langmuir*, 1993, **9**, 2820-2824.
44. L. D. Giddings and S. V. Olesik, *Langmuir*, 1994, **10**, 2877-2883.
45. O. Fernando Silva, M. A. Fernandez, J. J. Silber, R. H. de Rossi and N. Mariano Correa, *ChemPhysChem*, 2012, **13**, 124-130.
46. O. F. Silva, R. H. de Rossi and N. M. Correa, *RSC Adv.*, 2015, **5**, 34878-34884.
47. R. D. Falcone, N. M. Correa, M. A. Biasutti and J. J. Silber, *Langmuir*, 2000, **16**, 3070-3076.
48. B. Baruah, J. M. Roden, M. A. Sedgwick, N. M. Correa, D. C. Crans and N. E. Levinger, *J. Am. Chem. Soc.*, 2006, **128**, 12758-12765.
49. N. M. Correa, J. J. Silber, R. E. Riter and N. E. Levinger, *Chem. Rev.*, 2012, **112**, 4569-4602.
50. N. A. Vodolazkaya, N. O. Mchedlov-Petrosyan, N. V. Salamanova, Y. N. Surov and A. O. Doroshenko, *J. Mol. Liq.*, 2017, **157**, 105-112.
51. N. A. Vodolazkaya, Y. A. Kleshchevnikova and N. O. Mchedlov-Petrosyan, *J. Mol. Liq.*, 2017, **187**, 381-388.
52. D. C. Crans, S. Schoeberl, E. Gaidamauskas, B. Baruah and D. A. Roess, *J. Biol. Inorg. Chem.*, 2011, **16**, 961-972.
53. A. G. Sostarec, E. Gaidamauskas, S. Distin, S. J. Bonetti, N. E. Levinger and D. C. Crans, *Chem. Eur. J.*, 2014, **20**, 5149-5159.
54. G. R. Willsky, L.-H. Chi, M. Godzala, III, P. J. Kostyniak, J. J. Smee, A. M. Trujillo, J. A. Alfano, W. Ding, Z. Hu and D. C. Crans, *Coord. Chem. Rev.*, 2011, **255**, 2258-2269.
55. M. Li, W. Ding, J. J. Smee, B. Baruah, G. R. Willsky and D. C. Crans, *BioMetals*, 2009, **103**, 585-905.
56. D. C. Crans, *J. Org. Chem.*, 2015, **80**, 11899-11915.
57. T. Scior, J. A. Guevara-Garcia, Q.-T. Do, P. Bernard and S. Laufer, *Curr. Med. Chem.*, 2016, **23**, 2874-2891.
58. D. Sanna, J. Palomba, G. Lubinu, P. Buglyo, S. Nagy, F. Perdih and E. Garrriba, *J. Med. Chem.*, 2019, **62**, 654-664.
59. C. Milsmann, A. Levina, H. H. Harris, G. J. Foran, P. Turner and P. A. Lay, *Inorg. Chem.*, 2006, **45**, 4743-4754.
60. D. Sanna, V. Ugone, A. Fadda, G. Micera and E. Garrriba, *J. Inorg. Biochem.*, 2016, **161**, 18-26.
61. T. Jakusch, E. A. Enyedy, K. Kozma, Z. Paar, A. Benyei and T. Kiss, *Inorg. Chim. Acta*, 2014, **420**, 92-102.
62. Z. Chi, L. Zhu, X. Lu, H. Yu and B. Liu, *Z. Anorg. Allg. Chem.*, 2012, **638**, 1523-1530.
63. Z. Chi, L. Zhu and X. Lu, *J. Mol. Struct.*, 2011, **1001**, 111-117.
64. I. E. Leon, J. F. Cadavid-Vargas, I. Tiscornia, V. Porro, S. Castelli, P. Katkar, A. Desideri, M. Bollati-Fogolin and S. B. Etcheverry, *J. Biol. Inorg. Chem.*, 2015, **20**, 1175-1191.
65. V. Rajendiran, R. Karthik, M. Palaniandavar, H. Stoeckli-Evans, V. S. Periasamy, M. A. Akbarsha, B. S. Srinag and H. Krishnamurthy, *Inorg. Chem.*, 2007, **46**, 8208-8221.
66. C. R. Cornman, G. J. Colpas, J. D. Hoeschele, J. Kampf and V. L. Pecoraro, *J. Am. Chem. Soc.*, 1992, **114**, 9925-9933.
67. X. Li, M. S. Lah and V. L. Pecoraro, *Inorg. Chem.*, 1988, **27**, 4657-4664.
68. D. C. Crans, *Comments Inorg. Chem.*, 1994, **16**, 1-33.
69. A. Maitra, *J. Phys. Chem.*, 1984, **88**, 5122-5125.
70. M. Le, O. Rathje, A. Levina and P. A. Lay, *J. Biol. Inorg. Chem.*, 2017, **22**, 663-672.
71. G. R. Willsky, D. A. White and B. C. McCabe, *J. Biol. Chem.*, 1984, **259**, 13273-13281.
72. H. Tominaga, M. Ishiyama, F. Ohseto, K. Sasamoto, T. Hamamoto, K. Suzuki and M. Watanabe, *Anal. Commun.*, 1999, **36**, 47-50.
73. R. Hamid, Y. Rotshteyn, L. Rabadi, R. Parikh and P. Bullock, *Toxicol. in Vitro*, 2004, **18**, 703-710.
74. M. D. Hall, K. A. Telma, K.-E. Chang, T. D. Lee, J. P. Madigan, J. R. Lloyd, I. S. Goldlust, J. D. Hoeschele and M. M. Gottesman, *Cancer Res.*, 2014, **74**, 3913-3922.
75. A. Levina, A. Mitra and P. A. Lay, *Metallomics: integrated biometal science*, 2009, **1**, 458-470.
76. X. G. Yang, K. Wang, J. F. Lu and D. C. Crans, *Coord. Chem. Rev.*, 2003, **237**, 103-111.
77. D. C. Crans, L. Q. Yang, J. A. Alfano, L. H. Chi, W. Z. Jin, M. Mahroof-Tahir, K. Robbins, M. M. Toloue, L. K. Chan, A. J. Plante, R. Z. Grayson and G. R. Willsky, *Coord. Chem. Rev.*, 2003, **237**, 13-22.
78. D. C. Crans, *J. Inorg. Biochem.*, 2000, **80**, 123-131.
79. X. G. Yang, X. D. Yang, L. Yuan, K. Wang and D. C. Crans, *Pharm. Res.*, 2004, **21**, 1026-1033.
80. K. Thompson and C. Orvig, *J. Inorg. Biochem.*, 2006, **100**, 1925-1935.
81. D. Rehder, *Future Med. Chem.*, 2012, **4**, 1823-1837.
82. N. D. Chasteen, *Copper, Molybdenum, and Vanadium in Biological Systems*, Springer, 1983.
83. E. Alessio and L. Messori, in *Metallo-Drugs: Development and Action of Anticancer Agents*, eds. A. Sigel, H. Sigel, E. Freisinger and R. Sigel, 2018, pp. 141-170.
84. A. Levina, J. B. Aitken, Y. Y. Gwee, Z. J. Lim, M. Liu, A. M. Singharay, P. F. Wong and P. A. Lay, *Chem. Eur. J.*, 2013, **19**, 3609-3619.
85. S. Thota, D. A. Rodrigues, D. C. Crans and E. J. Barreiro, *J. Med. Chem.*, 2018, **61**, 5805-5821.
86. G. R. Willsky, L.-H. Chi, M. Godzala, III, P. J. Kostyniak, J. J. Smee, A. M. Trujillo, J. A. Alfano, W. Ding, Z. Hu and D. C. Crans, *Coord. Chem. Rev.*, 2011, **255**, 2258-2269.
87. X. Niu, R. Xiao, N. Wang, Z. Wang, Y. Zhang, Q. Xia and X. Yang, *Curr. Top. Med. Chem.*, 2016, **16**, 811-822.
88. C. C. McLauchlan, B. J. Peters, G. R. Willsky and D. C. Crans, *Coord. Chem. Rev.*, 2015, **301**, 163-199.
89. B. I. Posner, R. Faure, J. W. Burgess, A. P. Bevan, D. Lachance, G. Zhang-Sun, I. G. Fantus, J. B. Ng, D. A. Hall, B. Soo Lum and A. Shaver, *J. Biol. Chem.*, 1994, **269**, 4596-4604.
90. G. Sciortino, D. Sanna, V. Ugone, G. Micera, A. Lledos, J.-D. Marechal and E. Garrriba, *Inorg. Chem.*, 2017, **56**, 12938-12951.
91. T. Kiss, T. Jakusch, D. Hollender, Á. Dörnyei, É. A. Enyedy, J. C. Pessoa, H. Sakurai and A. Sanz-Medel, *Coord. Chem. Rev.*, 2008, **252**, 1153-1162.
92. A. Dornyei, S. Marcao, J. C. Pessoa, T. Jakusch and T. Kiss, *Eur. J. Inorg. Chem.*, 2006, **18**, 3614-3621.
93. D. Sanna, V. Ugone, P. Buglyo, S. Nagy, I. Kacsir and E. Garrriba, *Inorg. Chim. Acta*, 2018, **472**, 127-138.
94. D. Sanna, M. Serra, G. Micera and E. Garrriba, *Inorg. Chem.*, 2014, **53**, 1449-1464.
95. K. A. Doucette, K. N. Hassell and D. C. Crans, *J. Inorg. Biochem.*, 2016, **165**, 56-70.
96. S. A. Dikanov, B. D. Liboiron and C. Orvig, *J. Am. Chem. Soc.*, 2002, **124**, 2969-2978.
97. J. C. Pessoa and I. Tomaz, *Curr. Med. Chem.*, 2010, **17**, 3701-3738.
98. Y. Yoshikawa, H. Sakurai, D. C. Crans, G. Micera and E. Garrriba, *Dalton Trans.*, 2014, **43**, 6965-6972.
99. N. Samart, C. N. Beuning, K. J. Haller, C. D. Rithner and D. C. Crans, *Langmuir*, 2014, **30**, 8697-8706.
100. P. K. Glasoe and F. A. Long, *J. Phys. Chem.*, 1960, **64**, 188-190.
101. A. Levina, H. H. Harris and P. A. Lay, *J. Am. Chem. Soc.*, 2007, **129**, 1065-1075.
102. R. I. Freshney, *Culture of Animal Cells: A Manual of Basic Technique and Specialized Applications*, Wiley-Blackwell, Hoboken, NJ, 7th edn., 2016.
103. N. Schweigert, A. J. B. Zehnder and R. I. L. Eggen, *Environ. Microbiol.*, 2001, **3**, 81-91.
104. N. Pooransingh-Margolis, R. Renirie, Z. Hasan, R. Wever, A. J. Vega and T. Polenova, *J. Am. Chem. Soc.*, 2006, **128**, 5190-5208.
105. M. Zizic, Z. Miladinovic, M. Stanic, M. Hadzibrahimovic, M. Zivic and J. Zakrzeksa, *Res. Microbiol.*, 2016, **167**, 521-528.

## ARTICLE

## Dalton Transactions

106. B. J. Peters, A. S. Groninger, F. L. Fontes, D. C. Crick and D. C. Crans, *Langmuir*, 2016, **32**, 9451-9459.
107. M. Timm, L. Saaby, L. Moesby and E. W. Hansen, *Cytotechnology*, 2013, **65**, 887-894.
108. Microcal Ltd. Microcal Origin Version 6.1. Northampton MA USA.



“Hydrophobicity may increase hydrolytic stability of vanadium(V) catecholate complexes enabling rapid cellular uptake of intact complex exhibiting potent anti-cancer activity.”